

Autoionization-Detected Infrared Spectroscopy of Jet-Cooled Naphthol Cations

Eiji Fujimaki, Yoshiteru Matsumoto, Asuka Fujii,* Takayuki Ebata, and Naohiko Mikami*

Department of Chemistry, Graduate School of Science, Tohoku University, Sendai 980-8578, Japan

Received: March 2, 2000; In Final Form: June 5, 2000

We applied autoionization-detected infrared (ADIR) spectroscopy in order to observe OH stretching vibrations of jet-cooled 1- and 2-naphthol cations. In this technique, high Rydberg states, the vibrational levels of which are essentially the same as those of the corresponding bare molecular ion, were prepared by two-color double-resonance excitation. Vibrational transitions in the ion core of the high Rydberg states were measured by detecting the vibrational autoionization signal. For rotational and structural isomers of naphthol, similar low-frequency shifts of the OH frequencies upon ionization were found. The OH frequency shifts of naphthols were much smaller than that found for phenol, although both molecules have quite similar OH frequencies in their neutral ground state. This remarkable difference in frequency shifts was qualitatively explained in terms of the charge delocalization in the aromatic ring. In addition, the OH stretching vibrations of the 1- and 2-naphthol–Ar cluster cations were observed by infrared photodissociation spectroscopy. It was found that perturbations from the Ar atom to the hydroxyl group of naphthol are negligible in both the neutral and cationic ground states.

I. Introduction

Characteristic vibrational frequencies of functional groups are fundamental information in chemistry. In the case of neutral molecules, characteristic vibrational frequencies have been clearly established, based on extensive infrared (IR) and Raman spectroscopic studies.¹ On the other hand, our knowledge of the vibrational frequencies of molecular cations is still very slight, due to experimental difficulties in applying conventional spectroscopic techniques to these cations.²

Recently, we developed a new IR spectroscopic technique called autoionization-detected infrared (ADIR) spectroscopy, which is suitable for molecular cations prepared in a jet expansion.^{3–8} We applied this technique in order to observe the OH stretching vibrations of the phenol cation.^{3,6} It was found that the OH frequency of phenol was significantly reduced upon ionization ($\Delta\nu_{\text{OH}} = -123 \text{ cm}^{-1}$). We also measured the OH frequencies of several cations of phenol derivatives, including fluorophenol, cresol, ethylphenol, and methoxyphenol.^{6,8} Although those of the phenol derivatives showed similar low-frequency shifts upon the ionization, the magnitude of the low-frequency shift varied widely among molecules. Fluorophenol, cresol, and ethylphenol showed OH frequency shifts similar to that of phenol ($\Delta\nu_{\text{OH}} = 104\text{--}118 \text{ cm}^{-1}$), whereas the shifts of methoxyphenol were much smaller ($\Delta\nu_{\text{OH}} = 65\text{--}88 \text{ cm}^{-1}$). Gerhards et al. recently developed another new IR spectroscopic technique (IR–PIRI spectroscopy) for jet-cooled molecular cations, with which they observed the OH stretching vibrations of the resorcinol (1,3-dihydroxybenzene) cations.^{9,10} Resorcinol showed a behavior similar to that of methoxyphenol: its OH frequency shifts ($\Delta\nu_{\text{OH}} = 75\text{--}88 \text{ cm}^{-1}$) are much smaller than that of phenol. In contrast, the OH frequencies of these compounds in their neutral ground state (S_0) are quite comparatively similar; the largest difference among the phenol derivatives in S_0 is found to be only 10 cm^{-1} . Thus, the variety of OH frequencies of phenol derivatives in the cationic ground state (D_0) presents a sharp contrast with the similarity of their OH frequencies in S_0 .

The remarkable variety of OH frequencies among the phenol derivative cations suggests that the OH frequency is very sensitive to the electronic structure of the aromatic ring to which the hydroxyl group is bound. With respect to this, we investigated the OH stretching vibrations of jet-cooled 1- and 2-naphthol in S_0 and D_0 by using infrared–ultraviolet (IR–UV) double-resonance spectroscopy^{11–19} and ADIR spectroscopy,^{3–8} respectively. We compared the OH frequency shifts of naphthol upon ionization to those observed in the phenol derivatives and discussed the origin of the variety of the OH stretching frequencies in aromatic cations.

In addition, we applied the infrared photodissociation (IRPD) spectroscopic technique in order to observe the OH stretching vibrations of 1- and 2-naphthol–Ar cluster cations. In this technique, IR absorption is detected as the depletion of the cluster cation intensity, which is induced by vibrational predissociation of the cluster cation.^{7,20–24} The Ar atom plays the role of “messenger” in the IR absorption and enables us to detect IR absorption with high sensitivity. IRPD spectra obtained by this method are compared with the ADIR spectra of the corresponding bare cations, and perturbations from the Ar atom to the OH stretching vibration are examined.

II. Experiment

The OH stretching vibrations of jet-cooled naphthol and its Ar clusters in S_0 are observed by IR–UV spectroscopy. The ADIR and IRPD spectroscopic techniques are employed to measure the OH stretching vibrations of the bare cation and Ar cluster cation, respectively. All of these techniques are described elsewhere in detail;^{3,6,7,14} only a brief description is given herein.

A. IR–UV Double-Resonance Spectroscopy for the Neutral Ground State. A UV laser pulse of a wavelength that is fixed at the origin band of the S_1 – S_0 transition of the molecule (cluster) is introduced, and the resonance-enhanced multiphoton ionization (REMPI) signal is monitored as a measure of the population in S_0 . An IR laser pulse is introduced prior to the UV laser pulse, and its wavelength is scanned. When the IR

laser frequency is resonant with the OH stretching vibration of the molecule (cluster) in S_0 , reduction of the vibrational ground-state population occurs, and the depletion of the REMPI signal intensity is observed.

B. ADIR Spectroscopy for Molecular Cations in the Electronic Ground State. ADIR spectroscopy is an application of the concept of photoinduced Rydberg ionization (PIRI) spectroscopy, which has previously been used to observe electronic transitions of molecular cations.^{25–29} Very high Rydberg states ($n = 80–100$) of the molecule converging on the vibrationless level ($v = 0$) of the electronic ground state of the cation are prepared by two-color double-resonance excitation via the $S_1–S_0$ transition. The structure of the ion core of the Rydberg molecule can be regarded as the same as that of the bare molecular ion. An IR laser pulse is introduced a few nanoseconds after the excitation of the Rydberg states, and its wavelength is scanned. When the IR laser excites the vibration of the ion core, the total (=electronic and vibrational) energy of the Rydberg states exceeds the first ionization threshold, and vibrational autoionization occurs. By monitoring the ion current, an IR spectrum of the ion core, which can be regarded as corresponding to that of the bare cation, is observed. A pulsed electronic field is used to extract the ions into a time-of-flight mass spectrometer.

C. IRPD Spectroscopy for Cluster Cations in the Electronic Ground State. The naphthol–Ar 1:1 cluster cation is produced by using two-color ($1 + 1'$) REMPI of the corresponding neutral cluster. The first UV laser excites the neutral cluster to the zero vibrational level of S_1 , and the second UV laser ionizes it. The internal energy of the prepared cluster cation is suppressed below 300 cm^{-1} . After the delay time of 50 ns, the IR laser is introduced. When the IR laser wavelength is resonant with the vibrational transition of the ion core of the cluster cation, the vibrational excitation induces the vibrational predissociation of the cluster cation, which results in the depletion of the cluster ion intensity. By monitoring the cluster ion intensity while the IR wavelength is being scanned, the IR spectrum of the cluster cation is obtained as the depletion spectrum.

In all of the experiments above, the gaseous mixture of the sample vapor and He (or Ar) was expanded into a vacuum chamber through a pulsed valve, then skimmed by a skimmer 2 mm in diameter. The resulting molecular beam was introduced into the interaction region and irradiated by the lasers. A Wiley–McLaren-type time-of-flight mass spectrometer was used for the mass-separation of the resulting ions.³⁰ Typical background pressure of the chamber was 7×10^{-6} Torr. All samples were purchased from the Tokyo Kasei Co. and Aldrich and were used without further purification. All samples were heated to 350 K.

III. Results and Discussion

A. REMPI Spectra of Naphthols and Naphthol–Ar Clusters. Both 1- and 2-naphthol have *cis* and *trans* rotational isomers (rotamers), which arise from the conformation of the hydroxyl group. The definitions of these rotamers are schematically shown in Figure 1. Figure 2 shows the ($1 + 1'$) REMPI spectra of 1-naphthol and the 1-naphthol–Ar cluster around the origin band of the $S_1–S_0$ transition. Monitoring of the bare molecular cation ($m/e = 144$) reveals two bands, at 31 181 and 31 457 cm^{-1} , respectively. The jet-cooled $S_1–S_0$ spectrum of 1-naphthol has been well studied, and the two bands are assigned to the origin bands of the *cis* and *trans* monomers, respectively.^{31–33} The *cis* rotamer cannot be ionized by the one-color two-photon ($1 + 1$) photoabsorption via the origin band because

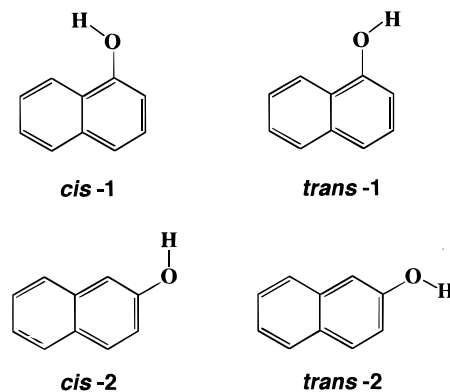


Figure 1. Schematic representations of the definitions of the rotational and structural isomers in naphthol.

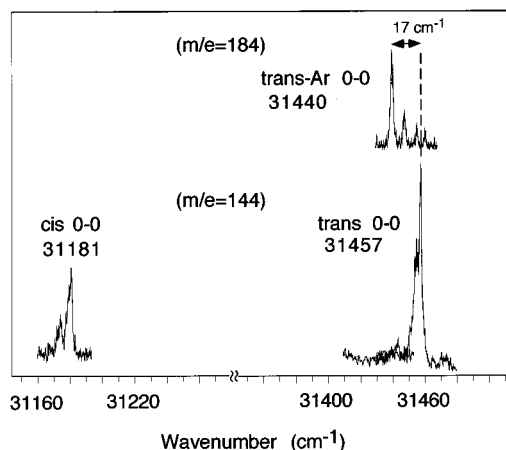


Figure 2. ($1 + 1'$) resonance-enhanced multiphoton ionization (REMPI) spectra of (lower trace) 1-naphthol and (upper trace) 1-naphthol–Ar around their origin bands of the $S_1–S_0$ transitions. In each spectrum, the monomer cation ($m/e = 144$) or the cluster cation ($m/e = 184$) is detected as a function of the first UV excitation laser wavelength. The 314 nm laser light was used to assist in the ionization.

its ionization potential ($62\,918\text{ cm}^{-1}$) is higher than the two-photon energy of the resonant photon.³⁴ We introduced another UV laser (314 nm) to assist in the ionization from S_1 .

Monitoring of the ion current intensity relative to the $m/e = 184$ cation reveals a band at $31\,440\text{ cm}^{-1}$, which is a 17 cm^{-1} low-frequency shift from the *trans* monomer. This band is clearly assigned to the origin band of the *trans*-1-naphthol–Ar cluster, and a short progression of an intermolecular vibration of 7 cm^{-1} appears on the high-frequency side. No band corresponding to the *cis*-1-naphthol–Ar cluster can be found. In 1-naphthol, the *trans* rotamer is more stable than the *cis* rotamer, and the ground-state population in the jet expansion prefers the *trans* rotamer. The Ar cluster intensity reflects the population of the corresponding monomer, whereas the population of the Ar cluster of the *cis* rotamer is too small to be detected.

Shown in Figure 3 are the mass-selected ($1 + 1'$) REMPI spectra of 2-naphthol and its Ar clusters around the origin bands of the $S_1–S_0$ transitions. The jet-cooled $S_1–S_0$ spectrum of bare 2-naphthol, in which bands appear at $30\,903$ and at $30\,585\text{ cm}^{-1}$, has been analyzed; the former band is attributed to the origin band of the *cis* rotamer, the latter to the *trans* rotamer.^{33,35} In the case of 2-naphthol, neither the *cis* nor the *trans* rotamers can be ionized by the ($1 + 1$) photoabsorption via their origin bands.³⁴ The 304 nm laser light was used to assist in the ionization from S_1 .

Monitoring of the Ar cluster cation ($m/e = 184$) reveals two extra bands near the origin bands of the *cis* and *trans* monomers.

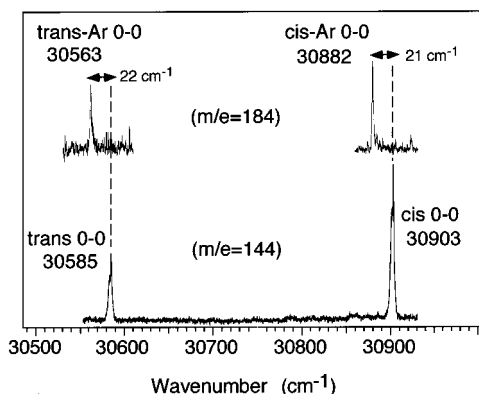


Figure 3. $(1 + 1')$ REMPI spectra of (lower trace) 2-naphthol and (upper trace) 2-naphthol-Ar around their origin bands of the S_1-S_0 transitions. In each spectrum, the monomer cation ($m/e = 144$) or the cluster cation ($m/e = 184$) is detected as a function of the first UV excitation laser wavelength. The 304 nm laser light was used to assist in the ionization.

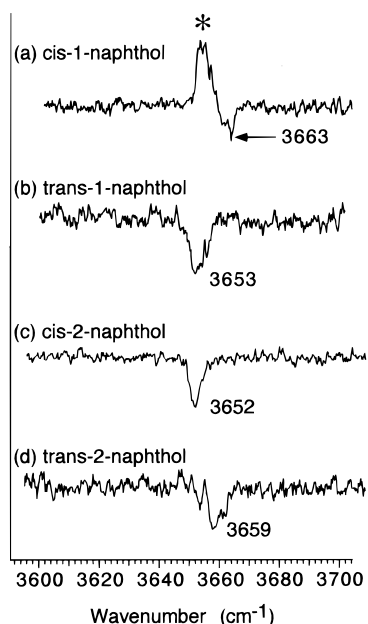


Figure 4. OH stretching vibrational region of infrared-ultraviolet (IR-UV) double-resonance spectra of (a) *cis*-1-naphthol, (b) *trans*-1-naphthol, (c) *cis*-2-naphthol, and (d) *trans*-2-naphthol in the neutral ground state (S_0). The asterisked peak seen in spectrum a is an artifact resulting from nonresonant ionization of the *trans* rotamer (see text).

These bands, at 30882 and 30563 cm^{-1} , are assigned to the origin bands of the *cis*-Ar and *trans*-Ar clusters, which show 21 and 22 cm^{-1} low-frequency shifts from the bands of the corresponding monomer, respectively.

B. OH Stretching Vibrations of Bare Naphthols in S_0 and D_0 . Figure 4 shows the OH stretch region of the IR-UV spectra of (a) *cis*-1-, (b) *trans*-1-, (c) *cis*-2-, and (d) *trans*-2-naphthol in the S_0 state. In each spectrum, the $(1 + 1')$ REMPI signal via the origin band of the S_1-S_0 transition is monitored, and the depletion of the ionization signal due to the IR absorption is recorded as a function of the IR wavelength. The observed OH frequencies are tabulated in Table 1. IR-UV spectroscopy has already been applied to the OH stretches of jet-cooled 1- and 2-naphthol, by Yoshino et al.¹⁷ and by our group,³⁶ respectively. Although the observed frequencies in the present measurements are slightly (2 cm^{-1}) smaller than those in the previous reports, except in the case of *trans*-1-naphthol, the present results essentially agree with those previous. We

TABLE 1: Observed and Calculated OH Stretching Vibrational Frequencies of 1- and 2-Naphthol and Phenol in S_0 and D_0 .^{a,b}

	S_0		D_0	
	observed	calculated ^c	observed	calculated ^c
<i>cis</i> -1-naphthol	3663			
<i>trans</i> -1-naphthol	3653	3697	3579	3642
<i>cis</i> -2-naphthol	3652	3663	3581	3626
<i>trans</i> -2-naphthol	3659	3663	3579	3627
phenol	3657 ^d	3666	3534 ^e	3580

^a In inverse centimeters ^b The density functional theoretical calculations were performed at the B3LYP/6-31G levels ^c Without frequency scaling. ^d From Tanabe et al.³⁷ ^e From Fujii et al.³

calibrated more carefully ($\pm 1 \text{ cm}^{-1}$ in the IR laser frequency and $\pm 1 \text{ cm}^{-1}$ in determination of the band center) and concluded that the present results are more reliable than those in our previous report.³⁶

The OH stretch bands of all of the neutral naphthol isomers appear in a similar region (3652–3663 cm^{-1}), and the frequency differences among the isomers are within 11 cm^{-1} . Therefore, it is concluded that the force field of the OH vibration in S_0 does not depend on the conformation, or the position of the substitution of the hydroxyl group. Moreover, the OH stretching frequency of bare phenol in S_0 is 3657 cm^{-1} ,³⁷ which falls just inside the aforementioned region. This suggests that OH frequencies of hydroxyaromatics in S_0 hardly depend on the size of the conjugated aromatic ring.

As indicated by an asterisk in the IR-UV spectrum of *cis*-1-naphthol in Figure 4a, a strong enhancement of the ionization signal is seen at 3653 cm^{-1} , which is the same as the OH frequency of the *trans* rotamer. Given that IR absorption results in a depletion of the ionization signal in IR-UV spectroscopy, this enhancement must be attributed to the nonresonant two-photon ionization following the IR absorption.³⁸ In the measurement of the IR-UV spectrum of the *cis* rotamer, the intensity of the first UV laser, the wavelength of which is fixed at the band origin of the *cis* rotamer, is much stronger than those used in the measurement of the *trans* rotamer, as a result of the much smaller population of the *cis* rotamer. Thus, the laser power is so intense that the nonresonant two-photon absorption is readily induced as soon as the two-photon energy exceeds the ionization threshold. The two-photon energy of the UV laser used for the transition starting from the zero point level, however, is not sufficient to ionize either of the rotamers. When the IR wavelength is resonant with the coexisting *trans* rotamer, the nonresonant two-photon excitation, starting from the vibrationally excited level, exceeds the first ionization threshold of the *trans* rotamer, leading to enhancement at the band position of the *trans* rotamer.

Shown in Figure 5 are the ADIR spectra of the cationic ground (D_0) state of (a) *trans*-1-, (b) *cis*-2-, and (c) *trans*-2-naphthol. In the case of *cis*-1-naphthol, the population in the jet expansion was so small that we could not detect its ADIR signal. The observed OH frequencies of the naphthol cations are tabulated in Table 1 and show that all of the OH frequencies of the isomer cations appear at $3580 \pm 1 \text{ cm}^{-1}$. This result indicates that the vibrational force field for the hydroxyl group in D_0 is quite similar among the structural and rotational isomer cations. It is also noted that the frequency reduction ($\Delta\nu_{\text{OH}}$) of naphthols upon the ionization is not large ($\Delta\nu_{\text{OH}} = 72\text{--}80 \text{ cm}^{-1}$), in compared with that of phenol ($\Delta\nu_{\text{OH}} = 123 \text{ cm}^{-1}$), although the OH frequencies of naphthols and phenol are very similar in S_0 .³

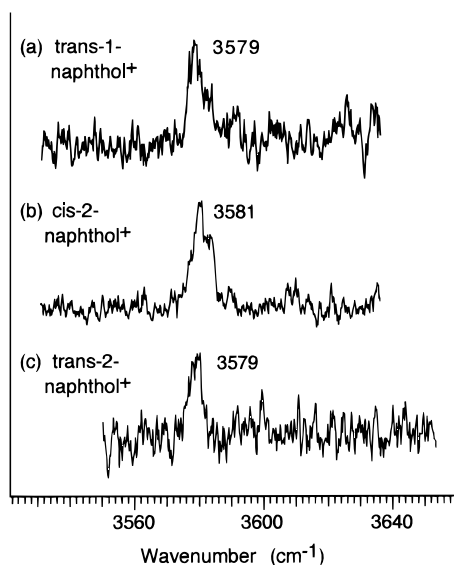


Figure 5. Autoionization-detected infrared (ADIR) spectra of (a) *trans*-1-naphthol, (b) *cis*-2-naphthol, and (c) *trans*-2-naphthol cations in the OH stretching vibrational region.

TABLE 2: OH Stretching Vibrational Frequencies of Hydroxyaromatics in S_0 and D_0 with Their Ionization Potentials^a

	isomer	S_0	D_0	$\Delta\nu_{\text{OH}}$	IP ₀
phenol		3657 ^b	3534 ^c	123	68 625 ^d
<i>m</i> -fluorophenol	<i>cis</i>	3659 ^e	3542 ^e	117	70 205 ^f
	<i>trans</i>	3658 ^e	3544 ^e	114	70 470 ^f
<i>p</i> -fluorophenol		3664 ^g	3546 ^e	118	68 560 ^f
<i>o</i> -cresol	<i>trans</i>	3655 ^h	3544 ^h	111	66 780 ^f
<i>m</i> -cresol	<i>cis</i>	3655 ^h	3544 ^h	111	66 810 ^f
	<i>trans</i>	3657 ^h	3545 ^h	112	66 960 ^f
<i>p</i> -cresol		3658 ^h	3551 ^h	107	65 925 ^f
<i>o</i> -ethylphenol	<i>trans</i>	3654 ^h	3545 ^h	109	66 500 ^f
<i>p</i> -ethylphenol		3658 ^h	3554 ^h	104	65 615 ^f
resorcinol	A	3657 ⁱ	3569 ^j	88	66 695 ⁱ
	B	3657 ⁱ	3582 ^j	75	
<i>m</i> -methoxyphenol	A	3657 ⁱ	3576 ^j	81	67 148 ⁱ
	B	3657 ^e	3584 ^e	73	65 230 ^f
<i>p</i> -methoxyphenol	A	3654 ^e	3589 ^e	65	64 740 ^f
	α	3662 ^e	3576 ^e	86	62 215 ^f
	β	3661 ^e	3573 ^e	88	62 310 ^f
1-naphthol	<i>trans</i>	3653 ^j	3579 ^j	74	62 637 ^k
2-naphthol	<i>cis</i>	3652 ^j	3580 ^j	72	63 670 ^k
	<i>trans</i>	3659 ^j	3579 ^j	80	63 189 ^k

^a In inverse centimeters. $\Delta\nu_{\text{OH}}$ is the OH frequency difference between S_0 and D_0 . The notation of the rotational isomers in resorcinol and methoxyphenol are taken from the references noted ^b From Tanabe et al.³⁷ ^c From Fujii et al.³ ^d From Dopfer and Müller-Dethlefs.⁴⁰ ^e From Fujimaki et al.⁶ ^f This work. The values include an experimental error of 15 cm⁻¹ (see text). ^g From Shitomi et al.³⁹ ^h From Fujimaki et al.⁸ ⁱ From Gerhards et al.^{9,10} ^j This work. ^k From Lakshminarayan et al.³⁴

C. Charge Delocalization Effects on the OH Stretching Frequencies in Hydroxyaromatic Cations. OH stretching vibrational frequency shifts upon ionization have recently been pointed out in reports on several phenol derivative cations studied by using the newly developed IR spectroscopic techniques for jet-cooled cations.^{6,8,9,10} Table 2 is a compilation of the observed OH frequencies of the phenol derivatives in S_0 and D_0 , together with those of naphthols. Because the ortho-substituted phenol derivatives involving intramolecular hydrogen bonding exhibit anomalous OH frequencies,⁴⁻⁶ such derivatives are excluded from the table. The following features are found in Table 2. (i) All of the OH frequencies in S_0 are similar (3652–3664 cm⁻¹). (ii) On the other hand, the OH frequencies

in D_0 are classified into two groups: the phenol, fluorophenol, cresol, and ethylphenol cations (hereafter we call group A) have relatively lower OH frequencies (around 3540 cm⁻¹), whereas the naphthol, resorcinol, and methoxyphenol cations (group B) show rather higher OH frequencies (around 3580 cm⁻¹). (iii) No significant difference in the OH frequencies is found between the meta and para structural isomers.

To understand the origin of the significant reduction of OH frequencies upon ionization, we performed density functional theoretical (DFT) calculations of phenol and naphthols by using the *Gaussian 94* program package with the B3LYP functionals and 6-31G basis set expansion.^{41,42} The calculated OH stretching frequencies of the energy optimized structures are tabulated in Table 1 along with the observed values. The key structural parameters concerning the hydroxyl group are compiled in Table 3. The calculated OH frequencies in their S_0 states agree well with the observed ones. Although the calculated OH frequencies in their D_0 are overestimated, the tendency of the phenol cation to show a much larger low-frequency shift than those of naphthol is qualitatively reproduced.

As seen in Table 3, structural changes upon the ionization are very similar among all of the isomers of naphthol and phenol; the O–H bond length becomes longer while the C–O bond is shortened and the C–O–H angle becomes larger. It is also noticed that a relatively larger change occurs in phenol, corresponding to the larger OH frequency shift. Such a structural deformation indicates that the contribution of the quinoid structure is enhanced as a result of the elimination of an electron from the aromatic ring.²⁴ This means that the positive charge produced in the aromatic ring attracts the electron density of the O–H bond into the ring, resulting in the reduction of the OH frequency. Thus, it is suggested that the variety of the OH frequencies in the hydroxyaromatic cations reflects the electronic structure of the aromatic ring, and especially its net charge. In fact, molecules of group B involve stronger electron-donating groups, such as hydroxyl or methoxyl groups, than those of group A (the methyl and ethyl groups or fluorine). In the resorcinol and methoxyphenol cations, therefore, the net charge of the aromatic ring is delocalized by the strong electron-donating group, resulting in relatively smaller OH frequency shifts upon ionization. In the case of the naphthol cations, the positive charge is delocalized in the whole area of the two aromatic rings, and the net charge per ring is therefore much smaller than those of the group A molecules. Such a charge delocalization effect is considered to be much less likely in S_0 because of the absence of the extra charge. This is consistent with the fact that group A and B molecules show similar OH frequencies in their S_0 state.

To confirm this interpretation of the OH frequency shift, we considered that it would be worthwhile to examine the correlation between ionization potentials and OH frequency shifts. Ionization potentials can be regarded as a measure of the stabilization due to the charge delocalization in aromatic cations, and their correlation to the OH frequency shifts is expected to provide experimental support for the above findings. The ionization potentials of the phenol derivatives are also tabulated in Table 2. The values of phenol, naphthol, and resorcinol were taken from the references of ZEKE spectroscopic studies,^{10,34,40} and those of the other molecules were measured by two-color ionization in our laboratory. Among the latter values, the experimental error due to field ionization of high Rydberg states is roughly estimated to be 15 cm⁻¹. A plot of the ionization potentials versus the OH frequency shifts is seen in Figure 6, showing that the group A molecules tend to have higher

TABLE 3: Calculated Key Structural Parameters Concerning the Hydroxyl Group of Naphthols and Phenol^a

		<i>trans</i> -1-naphthol	<i>cis</i> -2-naphthol	<i>trans</i> -2-naphthol	phenol
S ₀	r(C–O)/Å	1.3935	1.3992	1.3937	1.3938
	r(O–H)/Å	0.9759	0.9766	0.9761	0.9764
	θ(C–O–H)/°	111.49	111.66	111.68	111.63
D ₀	r(C–O)/Å	1.3486	1.3493	1.3497	1.3346
	r(O–H)/Å	0.9798	0.9801	0.9803	0.9841
	θ(C–O–H)/°	115.73	116.17	115.69	117.20

^a These values are based on the energy optimized structure in the B3LYP/6-31G calculations.

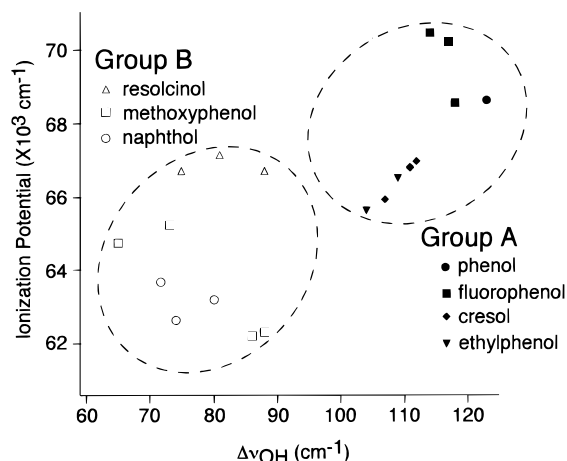


Figure 6. Correlation between the ionization potentials and shifts of the OH stretching frequencies upon ionization ($\Delta\nu_{\text{OH}}$).

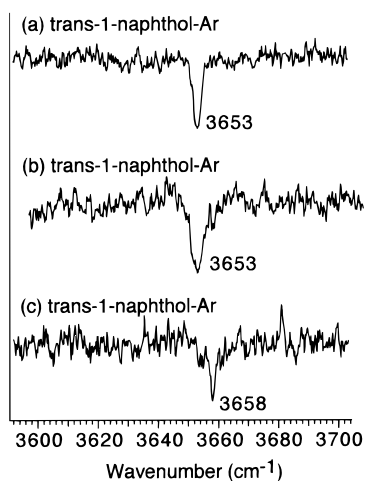


Figure 7. OH stretching vibrational region of IR–UV spectra of (a) *trans*-1-naphthol–Ar, (b) *cis*-2-naphthol–Ar, and (c) *trans*-2-naphthol–Ar in S₀.

ionization potentials than those of the group B molecules. The correlation between the ionization potentials and OH frequency shifts confirms that the charge delocalization of the aromatic ring strongly affects the OH frequency in the cationic state. However, the correlation is not so unequivocal as to be quantitative, and it should be noted that the charge delocalization would not be a unique factor for the OH frequency shift. The weak structural isomer dependence (i.e., the very small difference in the OH frequency shifts between the meta and para isomers) also indicates that the classical valence bond picture is not sufficient to explain the OH frequency shift. More elaborate analysis based on higher level ab initio calculations is required to fully elucidate the phenomenon. Such a detailed discussion will be reserved as the subject of future study.

D. OH Stretching Vibrations of Naphthol–Ar Clusters.

Figure 7 shows the IR–UV spectra of (a) *trans*-1-naphthol–

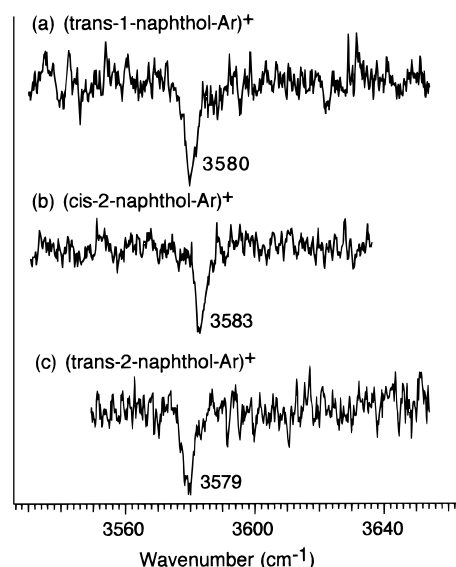


Figure 8. Infrared photodissociation (IRPD) spectra of (a) *trans*-1-naphthol–Ar, (b) *cis*-2-naphthol–Ar, and (c) *trans*-2-naphthol–Ar cations in the OH stretching vibrational region.

Ar, (b) *cis*-2-naphthol–Ar, and (c) *trans*-2-naphthol–Ar in S₀, each representing a OH frequency very similar to that of the corresponding monomer; their frequency differences are within 1 cm^{−1}. This fact indicates that the perturbation from the Ar atom to the hydroxyl group is essentially negligible. It is strongly suggested by this finding that the Ar atom places on the aromatic ring because such a cluster structure would minimize the perturbation to the in-plane vibrations including those in the OH mode.

Shown in Figure 8 are the IRPD spectra of (a) *trans*-1-naphthol–Ar, (b) *cis*-2-naphthol–Ar, and (c) *trans*-2-naphthol–Ar cations. As is the case in the neutral clusters, each isomer cluster cation also shows almost the same OH stretching frequency as that of the corresponding monomer cation, which was observed by ADIR spectroscopy. Their frequency differences are within 2 cm^{−1}, indicating that the perturbation of the Ar atom to the hydroxyl group is negligible even in the cations, although it is generally expected that interactions between the aromatic ring and rare gas atom increase upon the ionization.

These results strongly suggest that IRPD spectroscopy of aromatic–Ar cluster cations provides us with inherent spectroscopic information of the corresponding bare cations, as far as in-plane vibrations are concerned. In fact, such an equivalence between bare and Ar cluster cations has been confirmed for OH and CH stretching vibrations in phenol and its derivatives.^{3,7} The present results also prove the validity of IRPD spectroscopy of Ar cluster cation as a probe of the vibrational structure of the corresponding bare cation.

IV. Summary

The OH stretching vibrations of the rotamers of 1- and 2-naphthol cations were observed by using ADIR spectroscopy.

The low-frequency shifts of the OH stretching vibrations upon ionization were found. The magnitudes of the shifts are almost the same among all rotamers of 1- and 2-naphthol but are much smaller than that of phenol. The variety of OH frequencies in the hydroxyaromatic cations was qualitatively explained in terms of the charge delocalization in the aromatic ring.

IRPD spectroscopy was also performed for the naphthol–Ar cluster cations, and their OH stretching vibrations were observed. The cluster cations showed almost the same OH frequencies as those of the corresponding bare cations, indicating that the perturbation from the Ar atom to the hydroxyl group is negligible.

Acknowledgment. The authors gratefully acknowledge Drs. H. Ishikawa and T. Maeyama at Tohoku university and Dr. M. Gerhards at Heinrich-Heine Universität Düsseldorf for helpful discussions. This work was supported by JSPS Research for the Future Program “Photoscience”.

References and Notes

- (1) For example, see: Colthup, N. B.; Daly, L. H.; Wiberley, S. E. *Introduction to Infrared and Raman Spectroscopy*, 3rd ed.; Academic Press Inc.: San Diego, 1990.
- (2) Jacox, M. E. *J. Phys. Chem. Ref. Data* **1998**, *27*, 115.
- (3) Fujii, A.; Iwasaki, A.; Ebata, T.; Mikami, N. *J. Phys. Chem.* **1997**, *A101*, 5963.
- (4) Fujii, A.; Iwasaki, A.; Mikami, N. *Chem. Lett.* **1997**, 1099.
- (5) Fujii, A.; Fujimaki, E.; Ebata, T.; Mikami, N. *J. Am. Chem. Soc.* **1998**, *120*, 13256.
- (6) Fujimaki, E.; Fujii, A.; Ebata, T.; Mikami, N. *J. Chem. Phys.* **1999**, *110*, 4238.
- (7) Fujii, A.; Fujimaki, E.; Ebata, T.; Mikami, N. *Chem. Phys. Lett.* **1999**, *303*, 289.
- (8) Fujimaki, E.; Fujii, A.; Ebata, T.; Mikami, N. *J. Chem. Phys.* **2000**, *112*, 137.
- (9) Gerhards, M.; Schiwek, M.; Unterberg, C.; Kleinermanns, K. *Chem. Phys. Lett.* **1998**, *297*, 515.
- (10) Gerhards, M.; Unterberg, C.; Schumm, S. *J. Chem. Phys.* **1999**, *111*, 7966.
- (11) Page, R. H.; Shen, Y. R.; Lee, Y. T. *J. Chem. Phys.* **1988**, *88*, 5362.
- (12) Riehn, Ch.; Lahmann, Ch.; Wassermann, B.; Brutschy, B. *Chem. Phys. Lett.* **1992**, *197*, 443.
- (13) Zwier, T. S. *Annu. Rev. Phys. Chem.* **1996**, *47*, 205.
- (14) Ebata, T.; Fujii, A.; Mikami, N. *Int. Rev. Phys. Chem.* **1998**, *17*, 331.
- (15) Nakanaga, T.; Ito, F.; Miyawaki, J.; Sugawara, K.; Takeo, H. *Chem. Phys. Lett.* **1996**, *261*, 414.
- (16) Djafari, S.; Barth, H.-D.; Buchhold, K.; Brutschy, B. *J. Chem. Phys.* **1997**, *107*, 10573.
- (17) Yoshino, R.; Hashimoto, K.; Omi, T.; Ishiuchi, S.; Fujii, M. *J. Phys. Chem.* **1998**, *A102*, 6227.
- (18) Janzen, Ch.; Spangenberg, D.; Roth, W.; Kleinermanns, K. *J. Chem. Phys.* **1999**, *110*, 9898.
- (19) Graham, R. J.; Kroemer, R. T.; Mons, M.; Robertson, E. G.; Snoek, L. C.; Simons, J. P. *J. Phys. Chem.* **1999**, *A103*, 9706.
- (20) Okumura, M.; Yeh, L. I.; Myers, J. D.; Lee, Y. T. *J. Chem. Phys.* **1986**, *85*, 2328.
- (21) Fujii, A.; Sawamura, T.; Tanabe, S.; Ebata, T.; Mikami, N. *Chem. Phys. Lett.* **1994**, *225*, 104.
- (22) Satink, R. G.; Piest, H.; von Helden, G.; Meijer, G. *J. Chem. Phys.* **1999**, *111*, 10750.
- (23) Dopfer, O.; Olkhov, R. V.; Maier, J. P. *J. Chem. Phys.* **1999**, *111*, 10754.
- (24) Fujii, A.; Fujimaki, E.; Ebata, T.; Mikami, N. *J. Chem. Phys.* **2000**, *112*, 6275.
- (25) Taylor, D. P.; Goode, J. G.; LeClaire, J. E.; Johnson, P. M. *J. Chem. Phys.* **1995**, *103*, 6293.
- (26) Goode, J. G.; LeClaire, J. E.; Johnson, P. M. *Int. J. Mass Spectrom. Ion Processes* **1996**, *159*, 49.
- (27) LeClaire, J. E.; Anand, R.; Johnson, P. M. *J. Chem. Phys.* **1997**, *106*, 6785.
- (28) Anand, R.; Hofstein, J. D.; LeClaire, J. E.; Johnson, P. M. *J. Phys. Chem.* **1999**, *A103*, 8927.
- (29) Anand, R.; LeClaire, J. E.; Johnson, P. M. *J. Phys. Chem.* **1999**, *A103*, 2618.
- (30) Wiley, W. C.; McLaren, I. H. *Rev. Sci. Instrum.* **1955**, *26*, 1150.
- (31) Knochenmuss, R.; Cheshnovsky, O.; Leutwyler, S. *Chem. Phys. Lett.* **1988**, *144*, 317.
- (32) Knochenmuss, R.; Leutwyler, S. *J. Chem. Phys.* **1989**, *91*, 1268.
- (33) Johnson, J. R.; Jordan, K. D.; Plusquelic, D. F.; Pratt, D. W. *J. Chem. Phys.* **1990**, *93*, 2258.
- (34) Lakshminarayan, C.; Smith, J. M.; Knee, J. L. *Chem. Phys. Lett.* **1991**, *182*, 656.
- (35) Oikawa, A.; Abe, H.; Mikami, N.; Ito, M. *J. Phys. Chem.* **1984**, *88*, 5180.
- (36) Mastumoto, Y.; Ebata, T.; Mikami, N. *J. Chem. Phys.* **1998**, *109*, 6303.
- (37) Tanabe, S.; Ebata, T.; Fujii, M.; Mikami, N. *Chem. Phys. Lett.* **1993**, *215*, 347.
- (38) Omi, T.; Shitomi, H.; Sekiya, N.; Takazawa, K.; Fujii, M. *Chem. Phys. Lett.* **1996**, *252*, 287.
- (39) Shitomi, H.; Ishiuchi, S.; Fujii, M. *Abstract of the Conference on Molecular Structure* (Fukuoka, 1996).
- (40) Dopfer, O.; Müller-Dethlefs, K. *J. Chem. Phys.* **1994**, *101*, 8508.
- (41) Stevens, P. J.; Devlin, F. J.; Chablowski, C. F.; Frisch, M. J. *J. Phys. Chem.* **1994**, *98*, 11623.
- (42) Frisch, M. J.; Trucks, G. W.; Schlegel, H. B.; Gill, P. M. W.; Johnson, B. G.; Robb, M. A.; Cheeseman, J. R.; Keith, T.; Petersson, G. A.; Montgomery, J. A.; Raghavachari, K.; Al-Laham, M. A.; Zakrzewski, V. G.; Ortiz, J. V.; Foresman, J. B.; Cioslowski, J.; Stefanov, B. B.; Nanayakkara, A.; Challacombe, M.; Peng, C. Y.; Ayala, P. Y.; Chen, W.; Wong, M. W.; Andres, J. L.; Replogle, E. S.; Gomperts, R.; Martin, R. L.; Fox, D. J.; Binkley, J. S.; Defrees, D. J.; Baker, J.; Stewart, J. P.; Head-Gordon, M.; Gonzalez, C.; Pople, J. A. *Gaussian 94*, Revision D.4; Gaussian, Inc.: Pittsburgh, PA, 1995.